

Hubert Mayerhofer,^a
Gabriele Schramm,^b Georgios N.
Hatzopoulos,^a Christoph
Mueller-Dieckmann,^c Helmut
Haas^b and Jochen Mueller-
Dieckmann^{a*}

^aEMBL Hamburg Outstation, c/o DESY,
Notkestrasse 85, D-22603 Hamburg, Germany,

^bResearch Center Borstel, D-23845 Borstel,
Germany, and ^cESRF, 6 Rue Jules Horowitz,
F-38043 Grenoble CEDEX 09, France

Correspondence e-mail:
jochenmd@embl-hamburg.de

Received 10 February 2009
Accepted 28 April 2009

Cloning, expression, purification, crystallization and preliminary X-ray crystallographic analysis of interleukin-4-inducing principle from *Schistosoma mansoni* eggs (IPSE/alpha-1)

The interleukin-4-inducing principle from *Schistosoma mansoni* eggs (IPSE/alpha-1) triggers the release of large amounts of interleukin-4 from human blood basophils, thus presumably playing an immunomodulatory role during schistosome infection. IPSE/alpha-1 was crystallized and a native X-ray data set was collected to 1.66 Å resolution from a single crystal at 100 K using synchrotron radiation. The crystal belonged to space group $P6_1$ or $P6_5$, with one molecule per asymmetric unit.

1. Introduction

The trematode *Schistosoma mansoni* is a parasitic worm and the causative agent of schistosomiasis, also known as bilharzia or snail fever. This disease is second only to malaria in socioeconomic and public health importance. *S. mansoni* is found in Africa, the Middle East, the Caribbean and South America, where it is endemic, infecting about 200 million people in mostly rural areas (World Health Organization, 2007).

The life cycle of trematodes is complex and involves different hosts. The larvae hatch from eggs which are emitted into water along with faeces from their vertebrate hosts. The larvae of *S. mansoni* search for and infect water snails, which serve as intermediate hosts. Here, they multiply and mature into cercariae, the larval stage infective to humans. When the cercariae emerge from their intermediate host they actively search for their definitive host (humans). After penetrating human skin they transform into early mammalian-stage larvae (schistosomula), enter the circulatory system and mature into adult parasites. Those procreate sexually and produce eggs which are eventually released through the intestinal system.

Infection with *S. mansoni* triggers a reaction by the immune system. While juvenile and adult worms induce a T helper type 1 (Th1) response, schistosome eggs not only stimulate a T helper type 2 (Th2) reaction but also down-regulate Th1 and subsequently Th2 reactivity (Pearce & MacDonald, 2002). Thus, schistosome eggs have an immunomodulatory/anti-inflammatory effect. This effect strongly depends on the presence of interleukin-4 (IL-4) and IL-4 receptor signalling, since IL-4 and IL-4R α knockout mice die very early during schistosome infection owing to heavy and uncontrolled inflammation (Hoffmann *et al.*, 2000; Herbert *et al.*, 2004).

The active component in *S. mansoni* eggs which induces the release of IL-4 from human basophils (IPSE/alpha-1) has previously been isolated and characterized (Schramm *et al.*, 2003, 2006). It was further demonstrated that IPSE/alpha-1 triggers the release of IL-4 by binding to immunoglobulin E (IgE) bound to the cell-surface receptors of human basophils. However, the details of this interaction remain unknown. Determination of the three-dimensional structure of IPSE/alpha-1 is a first step towards the elucidation of this important and complex disease and immunoresponse mechanism.

IPSE/alpha-1 encodes 134 amino acids, including 20 N-terminal residues which are post-translationally removed in the mature protein. Similarity searches revealed no sequences with significant identity. Secondary-structure predictions indicate a mainly β -sheet-containing fold similar to that of γ -crystallin. In order to further



**Figure 1**

Top line: numbering of IPSE sequence in red. IPSE-SM denotes the protein sequence of IPSE based on its nucleotide sequence (GenBank accession No. AY028436), including a 20-amino-acid signal peptide (shown in bold) and a C-terminal nuclear localization sequence (NLS; boxed in grey). The mature protein from *S. mansoni* eggs starts at residue 21 and is shown in regular type (Schramm *et al.*, 2003). IPSEΔNLS corresponds to mature IPSE but lacks ten C-terminal amino acids starting at the NLS and carries an additional two residues at the N-terminus that remain after removal of the His tag.

functionally characterize IPSE/alpha-1, we intend to determine its three-dimensional structure by X-ray crystallography.

2. Materials and methods

2.1. Cloning, expression and purification

cDNA coding for IPSE/alpha-1 mutant IPSEΔNLS, which lacks ten amino acids at the C-terminus [including a seven-residue nuclear localization sequence (NLS) and a cysteine residue required for dimer formation of the native protein; Fig. 1], was amplified by PCR from IPSE/alpha-1 wild-type cDNA using the IPSE-specific primers (restriction sites shown in bold) *EheI*-sense, 5'-ATATAT**GGCG-CCGATTCATGCAAATATTGT**-3', and *HindIII*-antisense, 5'-AT-ATATA**AAGCTTTCATCATTGATTGATACATTCAAC**-3', and the following protocol: 30 cycles of denaturation at 368 K for 30 s, annealing at 331 K for 30 s and extension at 345 K for 1 min. PCR products were then cloned *via* the restriction sites *EheI* and *HindIII* into the expression vector pProExHTb (Gibco).

IPSEΔNLS was expressed as His-tagged fusion protein and purified mainly according to the protocol described previously for native IPSE/alpha-1 (Schramm *et al.*, 2003) with the following modifications. Expression was performed in *Escherichia coli* BL21 freshly transformed with the expression plasmid pProExHTb-IPSEΔNLS. The purified refolded protein was dialysed against phosphate-buffered saline (PBS; 137 mM NaCl, 2.7 mM KCl, 10 mM Na₂HPO₄, 1.7 mM KH₂PO₄) pH 8.5. The His tag was removed using AcTEV protease that was His-tagged itself (Invitrogen) at a concentration of 10 U AcTEV protease per 100 μg protein. Following cleavage (4 h at 303 K), IPSEΔNLS was separated from cleaved His tag and His-tagged AcTEV protease by Ni-NTA affinity chromatography in buffer A (50 mM Na₂HPO₄, 300 mM NaCl, 12.5 mM imidazole pH 8.0). The pure sample was then stored in PBS pH 7.0.

2.2. Crystallization

The purified protein solution was concentrated to 14 mg ml⁻¹ by centrifugation using an Amicon Ultra Centrifugal filter device (10 kDa molecular-weight cutoff; Millipore). Initial crystallization trials were carried out with six different 96-well screens from Hampton Research (Index, SaltRx and Crystal Screens 1 and 2), Jena Biosciences (Screens 1–8 with 24 conditions each) and Qiagen (ComPasSuite) at the EMBL Hamburg high-throughput crystallization facility (Mueller-Dieckmann, 2006). All initial screens were performed at 293 K in 96-well Greiner plates using the sitting-drop vapour-diffusion method. 300 nl protein solution was mixed with 300 nl reservoir solution and equilibrated against 50 μl reservoir

solution. Several conditions yielded microcrystalline material and the following two conditions resulted in small crystals: 0.2 M MgCl₂, 25% PEG 3350, 0.1 M Tris pH 8.5 and 20% 2-propanol, 10% PEG 4000. Crystals suitable for data collection were obtained through a combination of OptiSalt screening (Qiagen) and customized grid screens. The introduction of NaF from OptiSalts together with a search of various PEGs at different concentrations resulted in well diffracting but poorly shaped rod-like crystals (Fig. 2). These crystals were produced from 30 mM NaF, 15% 2-propanol and 8% PEG 1000 in 24-well plates by mixing 1.2 μl sample solution with 1 μl reservoir solution and equilibrating against 1 ml reservoir solution. Crystals appeared after at least one week and grew to dimensions of about 180 × 60 × 60 μm (Fig. 2).

2.3. Collection and processing of diffraction data

Prior to data collection, a single crystal was immersed for about 35 s in mother liquor augmented with 15% glycerol as a cryoprotectant. The crystal was then flash-cooled to 77 K in liquid nitrogen. A complete X-ray diffraction data set was collected on beamline ID29 at the ESRF (Grenoble, France) using an ADSC Q315R detector. A total of 120 frames were collected with a rotation range of 1.1° based on the prediction of *BEST* (Popov & Bourenkov, 2003). The data were indexed and integrated using *DENZO* and scaled with *SCALEPACK* (Otwinowski & Minor, 1997). Intensities were converted to structure-factor amplitudes using the program *TRUNCATE* (French & Wilson, 1978; Collaborative Computational Project, Number 4, 1994). Table 1 summarizes the data-collection and

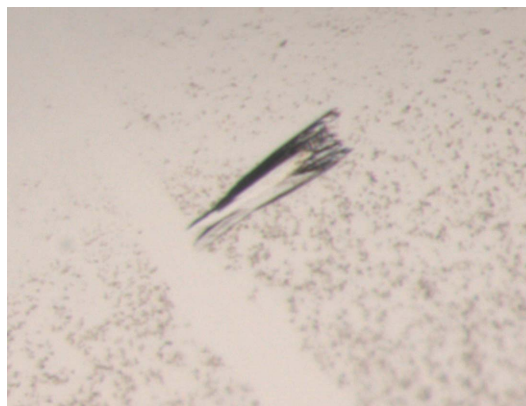


Figure 2
Crystal of IPSEΔNLS from *S. mansoni*.

Table 1

X-ray data-collection and processing statistics.

Values in parentheses are for the highest resolution shell.

X-ray source	ID29, ESRF
Wavelength (Å)	0.9762
Space group	$P6_1$ or $P6_5$
Unit-cell parameters (Å, °)	$a = b = 54.40$, $c = 56.71$, $\gamma = 120$
Resolution range (Å)	99–1.66 (1.69–1.66)
Observed reflections	83352
Unique reflections	11138 (549)
R_{merge} (%)	10.8 (44.9)
Completeness (%)	98.2 (99.6)
$I/\sigma(I)$	22.8 (3.8)
Multiplicity	7.4 (4.0)
Wilson B factor (Å ²)	15.2
Optical resolution (Å)	1.33
Mosaicity (°)	0.4

processing statistics. The optical resolution was calculated using the program *SFHECK* (Vaguine *et al.*, 1999).

3. Results and discussion

Native IPSE/alpha-1 consists of 114 amino acids. The C-terminus contains a seven-residue nuclear localization sequence (NLS) plus another three amino acids including a Cys residue. This Cys residue can form an intermolecular disulfide bridge that results in the homodimerization of IPSE/alpha-1 (Schramm, 2008). The protein was expressed and purified as described previously with a cleavable His tag at the N-terminus (Schramm *et al.*, 2003). Different constructs with and without the N-terminal His tag and with and without the ten C-terminal residues were subjected to crystallization trials. Only the tag-free IPSE/alpha-1 construct without the ten C-terminal residues (IPSEΔNLS) yielded well diffracting crystals. Removal of the C-terminus does not influence the ability of IPSE/alpha-1 to bind to IgE (Schramm, 2008).

Initial crystals of IPSEΔNLS grew after 7–14 d in two different conditions (0.2 M MgCl₂, 25% PEG 3350, 0.1 M Tris pH 8.5 and 20% 2-propanol, 10% PEG 4000). Both conditions were subjected to optimization trials, combining use of the OptiSalt strategy (Qiagen) and customized screens. The best diffracting crystals grew in 30 mM NaF, 15% 2-propanol and 8% PEG 1000 from drops consisting of 1.2 μl sample solution and 1 μl reservoir solution equilibrated against 1 ml reservoir solution. The crystals exhibited an irregular shape with a roughly arrow-like or lance-like morphology (Fig. 2). While the tips of these crystals were usually compact, their ends were frayed. Nevertheless, these crystals diffracted X-ray radiation to beyond 1.7 Å resolution (Fig. 3). For data collection, the synchrotron beam (50 × 50 μm) was centred onto the compact-looking tip, avoiding the frayed end of the crystal.

Data were indexed in the hexagonal space group $P6_1$ or $P6_5$, with unit-cell parameters $a = b = 54.40$, $c = 56.71$ Å, $\alpha = \beta = 90$, $\gamma = 120^\circ$. The asymmetric unit contains one molecule based on a molecular weight of 11.8 kDa and a Matthews parameter of 1.93 Å³ Da⁻¹ (Matthews, 1968), which corresponds to a solvent content of 36%.

Sequence-similarity searches using *BLAST* do not reveal any significant hits other than from schistosomes. We will therefore

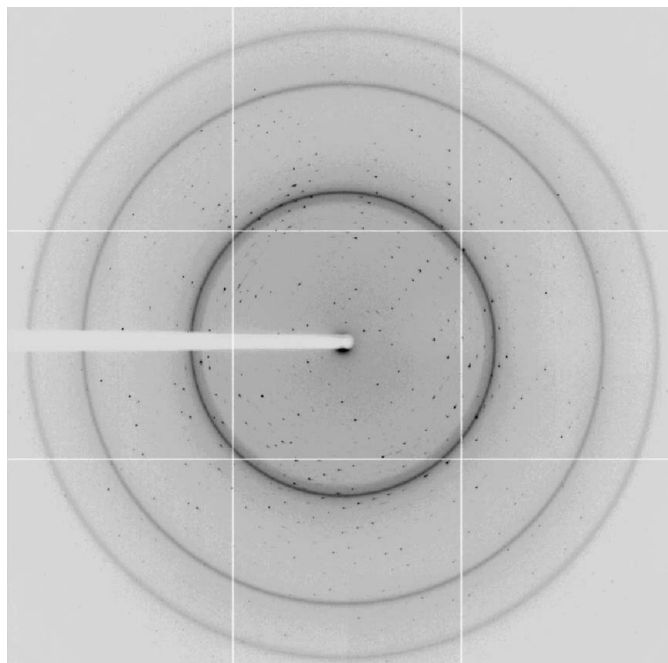


Figure 3

Diffraction pattern of an IPSEΔNLS crystal taken on beamline ID29 of the ESRF. The edge of the detector corresponds to a resolution of 1.7 Å.

attempt to solve the structure by phasing using S-SAD (ISPEΔNLS contains six S atoms) or MIR.

This work was supported by DFG SFB/TR22-TP A12.

References

- Collaborative Computational Project, Number 4 (1994). *Acta Cryst.* **D50**, 760–763.
- French, S. & Wilson, K. (1978). *Acta Cryst.* **A34**, 517–525.
- Herbert, D. R., Hölscher, C., Mohrs, M., Arendse, B., Schwegmann, A., Radwanska, M., Lesto, M., Kirsch, R., Hall, P., Mossmann, H., Claussen, B., Förster, I. & Brombacher, F. (2004). *Immunity*, **20**, 623–635.
- Hoffmann, K. F., Cheever, A. W. & Wynn, T. A. (2000). *J. Immunol.* **164**, 6406–6416.
- Matthews, B. W. (1968). *J. Mol. Biol.* **33**, 491–497.
- Mueller-Dieckmann, J. (2006). *Acta Cryst.* **D62**, 1446–1452.
- Otwinowski, Z. & Minor, W. (1997). *Methods Enzymol.* **276**, 307–326.
- Pearce, E. J. & MacDonald, A. S. (2002). *Nature Rev. Immunol.* **2**, 499–511.
- Popov, A. N. & Bourenkov, G. P. (2003). *Acta Cryst.* **D59**, 1145–1153.
- Schramm, G. (2008). Personal communication.
- Schramm, G., Falcone, F. H., Gronow, A., Haisch, K., Mamatt, U., Doenhoff, M. J., Oliveira, G., Galle, J., Dahinden, C. A. & Haas, H. (2003). *J. Biol. Chem.* **278**, 18384–18392.
- Schramm, G., Gronow, A., Knobloch, J., Wippersteg, V., Grevelding, C. G., Fuller, H., Stanley, R. G., Chioldini, P. L., Haas, H. & Doenhoff, M. J. (2006). *Mol. Biochem. Parasitol.* **147**, 9–19.
- Vaguine, A. A., Richelle, J. & Wodak, S. J. (1999). *Acta Cryst.* **D55**, 191–205.
- World Health Organization (2007). *2007 Schistosomiasis Facts*. Geneva, Switzerland: World Health Organization.